Ocular aberrations as a function of wavelength in the near infrared measured with a femtosecond laser

Enrique J. Fernández

Department of Biomedical Engineering and Physics, Medical University of Vienna, Vienna, Austria
Laboratorio de Optica, Departamento de Física, Universidad de Murcia, Campus de Espinardo (Ed. C), 30071 Murcia, Spain
enrique.fernandez@meduniwien.ac.at

Angelika Unterhuber

Department of Biomedical Engineering and Physics, Medical University of Vienna, Vienna, Austria
angelika.unterhuber@meduniwien.ac.at

Pedro M. Prieto

Laboratorio de Optica, Departamento de Física, Universidad de Murcia, Campus de Espinardo (Ed. C), 30071 Murcia, Spain
pegrito@um.es

Boris Hermann and Wolfgang Drexler

Department of Biomedical Engineering and Physics, Medical University of Vienna, Vienna, Austria
boris.hermann@meduniwien.ac.at, wolfgang.drexler@meduniwien.ac.at

Pablo Artal

Laboratorio de Optica, Departamento de Física, Universidad de Murcia, Campus de Espinardo (Ed. C), 30071 Murcia, Spain
pablo@um.es

Abstract: A compact mode-locked Ti:sapphire laser, emitting a broad spectrum of 277 nm bandwidth, centered at 790 nm, was used to measure the dependence of the aberrations of the human eye with wavelength in the near infrared region. The aberrations were systematically measured with a Hartmann-Shack wave-front sensor at the following wavelengths: 700, 730, 750, 780, 800, 850, 870 and 900 nm, in four normal subjects. During the measurements, the wavelengths were selected by using 10 nm band-pass filters. We found that monochromatic high order aberrations, beyond defocus, were nearly constant across 700 to 900 nm wavelength in the four subjects. The average chromatic difference in defocus was 0.4 diopters in the considered wavelength band. The predictions of a simple water-eye model were compared with the experimental results in the near infrared. These results have potential applications in those situations where defocus or higher order aberration correction in the near infrared is required. This is the case of many imaging techniques: scanning laser ophthalmoscope, flood illumination fundus camera, or optical coherence tomography.

OCIS codes: (330.5370) Physiological optics; (170.4460) Ophthalmic optics; (140.4050) Mode-locked lasers.

References and links

1. M. S. Smirnov, "Measurement of the wave aberration of the human eye," Biofizika **6**, 687-703 (1961).

#6061 - $15.00 US Received 14 December 2004; revised 5 January 2005; accepted 5 January 2005

2. B. Howland and H. C. Howland, "Subjective measurement of high order aberrations of the eye," Science **193**, 580-582 (1976).
3. G. Walsh, W. N. Charman, and H. C. Howland, "Objetive technique for the determination of monochromatic aberrations of the human eyes," J. Opt. Soc. Am. A **1**, 987-992 (1984).
4. J. Liang, B. Grimm, S. Goelz, and J. F. Bille, "Objective measurement of wave aberration of the human eye with the use of a Hartmann-Shack wave-front sensor," J. Opt. Soc. Am. A. **11**, 1949-1957 (1994).
5. I. Iglesias, E. Berrio, and P. Artal, "Estimates of the ocular wave aberration from pairs of double-pass retinal images," J. Opt. Soc. Am. A. **15**, 2466-2476 (1998).
6. P. Artal and A. Guirao, "Contributions of the cornea and the lens to the aberrations of the human eye," Opt. Lett. **23**, 1713-1715 (1998).
7. P. Artal, A. Guirao, E. Berrio, and D. R. Williams, "Compensation of corneal aberrations by the internal optics in the human eye," Journal of Vision **1**, 1-8 (2001), http://journalofvision.org/1/1/1.
8. G. Wald and D. R. Griffin, "The change in refractive power of the human eye in dim and bright light," J. Opt. Soc. Am. **37**, 321-336 (1947).
9. R. E. Bedford and G. Wyszecki, "Axial chromatic aberration of the human eye," J. Opt. Soc. Am. **47**, 564-565 (1957).
10. W. N. Charman and J. A. Jennings, "Objective measurements of the longitudinal chromatic aberration of the human eye," Vision Res. **16**, 999-1005 (1976).
11. P. A. Howarth and A. Bradley, "The longitudinal chromatic aberration of the human eye and its correction," Vision Res. **26**, 361-366 (1986).
12. Y. U. Ogboso and H. E. Bedell, "Magnitude of lateral chromatic aberration across the retina of the human eye," J. Opt. Soc. Am. A **4**, 1666-1672 (1987).
13. P. Simonet and M. C. W. Campbell, "The optical transverse chromatic aberration on the fovea of the human eye," Vision Res. **30**, 187-206 (1990).
14. L. N. Thibos, M. Ye, X. Zhang, and A. Bradley, "The chromatic eye: a new reduce-eye model of ocular chromatic aberration in humans," App. Opt. **31**, 592-599 (1992).
15. A. van Meeteren, "Calculations of the optical modulation transfer function of the human eye for white light," Opt. Acta **21**, 395-412 (1974).
16. S. Marcos, S. A. Burns, E. Moreno-Barriuso, and R. Navarro, "A new approach to study ocular chromatic aberrations," Vision Res. **39**, 4309-4323 (1999).
17. F. C. Delori and K. P. Pflibsen, "Spectral reflectance of the human ocular fundus," Appl. Opt. **28**, 1061-1067 (1989).
18. J. Santamaría, P. Artal, and J. Bescós, "Determination of the point-spread function of the human eye using a hybrid optical-digital method," J. Opt. Soc. Am. A **4**, 1109-1114 (1987).
19. N. López-Gil and P. Artal, "Comparison of double-pass estimates of the retinal image quality obtained with green and near-infrared light," J. Opt. Soc. Am. A **14**, 961-971 (1997).
20. L. Llorente, L. Díaz-Santana, D. Lara-Saucedo, and S. Marcos, "Aberrations of the human eye in visible and near infrared illumination," Optom. Vis. Sci. **80**, 26-35 (2003).
21. T. Fuji, A. Unterhuber, V. S. Yakovlev, G. Tempea, A. Stingl, F. Krausz, and W. Drexler, "Generation of smooth, ultra-broadband spectra directly from a prism-less Ti:sapphire laser," Appl. Phys. B **77**, 125–128 (2003).
22. P. M. Prieto, F. Vargas-Martín, S. Goelz, and P. Artal, "Analysis of the performance of the Hartmann-Shack sensor in the human eye," J. Opt. Soc. Am. A **17**, 1388-1400 (2000).
23. W. Drexler, U. Morgner, R. K. Ghanta, F. X. Kärtner, J. S. Schuman, and J. G. Fujimoto, "Ultrahigh-resolution ophthalmic optical coherence tomography," Nat. Med. **7**, 502-507 (2001).
24. H. Hofer, P. Artal, B. Singer, J. L. Aragon, and D. R. Williams, "Dynamics of the eye´s wave aberration," J. Opt. Soc. Am. A **18**, 1-10 (2001).
25. L. N. Thibos, A. Bradley, and X. Zhang, "The effect of ocular chromatic aberration on monocular visual performance," Optom. Vis. Sci. **68**, 599-607 (1991).
26. Y. Le Grand and S. G. El Hage, *Physiological Optics* (Springer-Verlag Berlin Heidelberg New York, 1980).
27. B. Hermann, E. J. Fernández, A. Unterhuber, H. Sattmann, A. F. Fercher, W. Drexler, P. M. Prieto, and P. Artal, "Adaptive Optics Ultrahigh Resolution Optical Coherence Tomography," Opt. Lett. **29**, 2142-2144 (2004)

1. Introduction

The aberrations of the human eye have been intensively studied in the last decades. Many different techniques have been proposed for measuring the monochromatic ocular aberrations, by means of both objective and subjective methods [1-5]. The two main contributors to the overall monochromatic aberrations in the human eye are the cornea and the crystalline lens [6,7]. Their surfaces and their internal refractive index distribution are the main responsible for the observed aberrations. Since the refractive index is a function of wavelength, the

#6061 - $15.00 US Received 14 December 2004; revised 5 January 2005; accepted 5 January 2005

monochromatic aberrations also depend on the considered wavelength. In particular, the chromatic dependence of focus, longitudinal chromatic aberration (LCA) [8-11] and the chromatic difference in magnification, transverse chromatic aberration (TCA) [12,13], have been measured in the eye. The LCA has been modeled by using relatively simple water-eye models [14]. The predictions of this model are in good agreement with the average LCA values obtained in the human eye in the visible range.

The change of high order aberrations with wavelength is expected to be modest in comparison with defocus. In fact, high order monochromatic aberrations have been traditionally assumed to remain nearly constant across the visible spectrum [15]. More recent experimental measurements obtained with a subjective procedure have revealed the validity of this assumption in the visible range [16].

All the existing knowledge on the ocular aberrations is, however, basically limited to the visible wavelengths. In particular, the chromatic dependence of aberrations in the near infrared (NIR) has not been studied so far, although this range is especially interesting to study the human eye. Ophthalmoscopes and other imaging techniques, as well as wave-front sensors, are currently operating with NIR illumination. One advantage of using NIR instead of visible light is the lower sensitivity of the human eye to the IR light, which renders the measurements more comfortable for the subjects. This also enables measurements without using any drugs to paralyze the accommodation or dilate the pupil. In addition, the human fundus has a higher reflectance in the NIR than in the visible [17]. Consequently, the amount of light required to both imaging the retina and measuring the aberrations is reduced, which is important to be within the safety maximum exposure limits.

Some previous studies compared the eye's optical quality at visible and NIR illumination. By using a double-pass technique [18], similar image quality at best focus was measured at 543 nm and 780 nm [19]. In a more recent paper [20], the high order aberrations measured at 543 nm and 787 nm were found to be also quite similar.

Systematic measurements of aberrations in the NIR have not been performed so far. Neither the dependence with wavelength of high order aberration nor defocus (LCA) has been characterized in this range. This might be due to the absence of appropriate light sources of high spatial coherence with reasonable intensity emitting in the NIR. A possible approach besides tunable lasers is the use of recently developed femtosecond ultra-broad band Ti:sapphire lasers [21]. These Kerr-lens mode-locked lasers enable the emission of smooth ultra-broad spectra in the NIR directly out of a compact, prism-less and user-friendly oscillator where no other light sources with comparable bandwidth, smooth spectrum and reliability are available.

In this paper, we combine for the first time this novel technology with a Hartmann-Shack wave-front sensor to systematically measure the ocular aberrations in the NIR part of the spectrum.

2. Methods

Ocular aberrations were objectively measured at different wavelengths, within the NIR range, by means of a Hartmann-Shack (H-S) wave-front sensor adapted for the human eye. The H-S sensor consisted of an IR CCD camera, providing good quantum efficiency for the range of interest, and a lenslet array (0.6 mm square lenses of 6.4 mm of focal length). This relatively short focal length enabled the microlenses array to be inserted into the CCD camera mounting, making the sensor compact. From the H-S images, the wave aberrations were calculated as previously described [22]. Figure 1 depicts the complete system with the main components. Lenses L1 and L2 (focal lengths 200 mm and 180 mm respectively) conjugate the eye's exit pupil with the lenslet array of the H-S wave-front sensor. These lenses are achromatic doublets, specifically designed for minimizing the chromatic aberrations in the NIR. Correct positioning of the eye was achieved by using the external camera CM1 and a flip mirror placed after L1. The objective of CM1 focuses to infinity so that the virtual image of the iris produced by the cornea is sharply imaged when it is exactly at the focal plane of L1. Subjects were fixed by using a bite-bar, where the mold of the dental impression of the user was

#6061 - $15.00 US Received 14 December 2004; revised 5 January 2005; accepted 5 January 2005

clamped to a 3-D positioning system, enabling the correct alignment of the pupil. The illumination source for the H-S sensor was a compact, prismless, mode-locked Ti:sapphire laser, emitting a smooth spectrum of 277 nm optical bandwidth (at full width at half maximum) centered at 790 nm. The same types of light sources have been also recently used in ultra-high resolution optical coherence tomography of the retina [23].

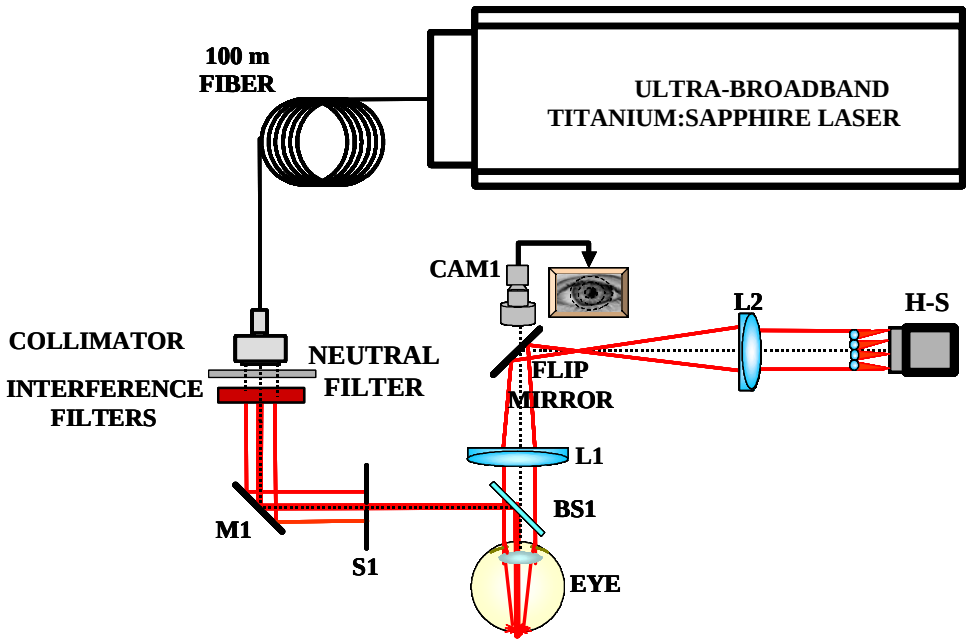

Fig. 1. Scheme of the experimental apparatus. The aberrations are measured by a Hartmann-Shack wave front sensor (HS) specifically designed for the human eye. The femtosecond mode-locked Ti:sapphire laser is coupled to the system through a 100-meters long fiber, preventing the existence of intensity peaks in the illumination beam. The different wavelengths in the NIR band are selected by means of a set of interference filters placed immediately behind the fiber's collimator. See text for a more detailed description of the experimental system and its operation.

In this study, we benefit from the emitted broad spectrum of these light sources by performing systematic measurements of the aberrations at the following wavelengths: 700, 730, 750, 780, 800, 850, 870 and 900 nm. The wavelengths were selected by means of 10 nm band-pass interference filters. For safety reasons, the ultra-short pulses were stretched by passing the beam through a 100-meters long fiber before entering the eye. The fiber output can be considered as a continuous wave, thus preventing potential damage of the ocular media due to high intensity peaks. Light from the femtosecond laser passed the interference filter, an appropriate neutral density filter and a 1 mm of diameter aperture that limited the size of the beam entering the eye, and reached the eye after reflection in a pellicle beam splitter BS1. A slight misalignment of the illumination beam with respect to the corneal apex prevents the corneal reflection to enter the HS camera, then affecting the measurements. Accommodation was paralyzed and pupil dilated by instilling two drops of tropicamide (0.5 %). The average exposure levels at the cornea were maintained below 1 μW. The light power was systematically measured and adjusted by means of neutral filters mounted on a wheel placed in front of the fiber exit. Four subjects participated in this study with ages ranging from 27 to 38 years. The experimental procedure was as follows: once the subject was centered with the help of camera CM1, the HS images over a 7 mm pupil were continuously recorded during 3

#6061 - $15.00 US Received 14 December 2004; revised 5 January 2005; accepted 5 January 2005

seconds at the selected wavelength. Since the H-S wave-front sensor operates in real time at 30 Hz, 90 independent frames were recorded. The measurements were repeated 3 times, therefore obtaining 270 estimates of the ocular aberrations on every selected wavelength, by placing the appropriate interference filter. The average aberration, at each wavelength, was then obtained by using the 270 ocular aberration estimates. Additionally, a set of measurements was recorded for broad-band illumination (without interference filters), allowing all the spectral components to reach the eye. The complete set of measurements in a subject took approximately one hour. The subjects were allowed to rest and leave the bite-bar between the runs.

3. Results

The mean aberrations at the selected wavelengths were calculated for every subject as the average across frames and runs. This averaging is intended to cancel out the rapid changes on the ocular aberrations [24]. The wave aberrations were expressed in terms of the Zernike polynomial expansion up to fifth order. Figure 2 shows a color-coded representation of the average wave-aberrations for each wavelength for all the subjects in a 7 mm diameter pupil, together with the obtained aberrations when all the spectral components illuminated simultaneously the eye (labeled in the figure as IR).

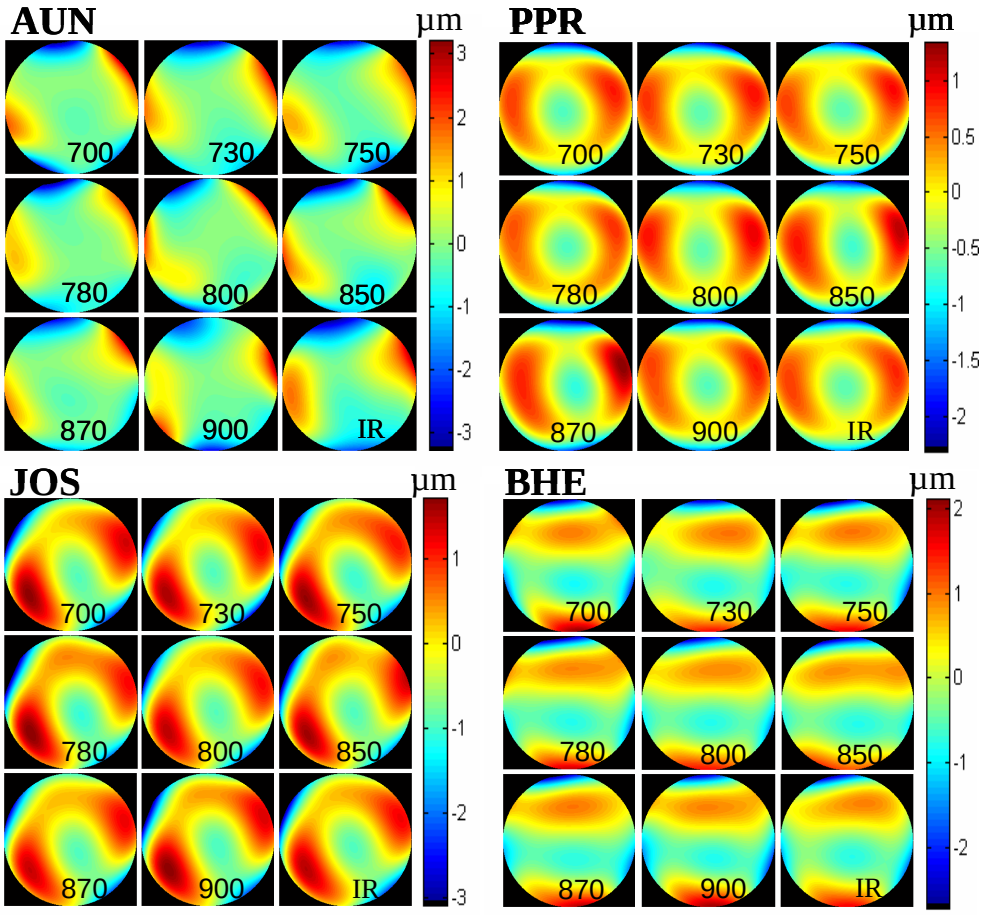

Fig. 2. Color-coded representations of the ocular aberrations (up to 5th order, excluding defocus) over a 7 mm diameter pupil as a function of the illumination wavelength. Wavelengths were selected by means of interference filters of 10 nm band-width. For each subject, bottom-right panel corresponds to broad-band illumination (no interference filter).

#6061 - $15.00 US Received 14 December 2004; revised 5 January 2005; accepted 5 January 2005

Defocus was not included in these wave-aberrations maps. Even in this color-coded representation, the differences between the wave-aberrations for the different wavelengths or with broad-band illumination are hardly noticeable. Although qualitatively, Fig. 2 indicates that higher order aberrations are practically independent on wavelength in the studied NIR range. In order to show these results more quantitatively, the evolution of some particular Zernike terms was analyzed. Figure 3 shows the astigmatism (Zernike Z_2^{-2} and Z_2^2, represented in the figure as squares), coma (polynomials Z_3^{-1} and Z_3^1 represented by circles) and the fourth-order spherical aberration (polynomial Z_4^0, triangles) as a function of wavelength. In all the cases, error bars show the standard deviation calculated from the whole set of experimental measurements obtained for each subject and wavelength. Figure 3 also includes the corresponding measured aberrations when using the broad-band spectrum illumination, as a separate, broader data point.

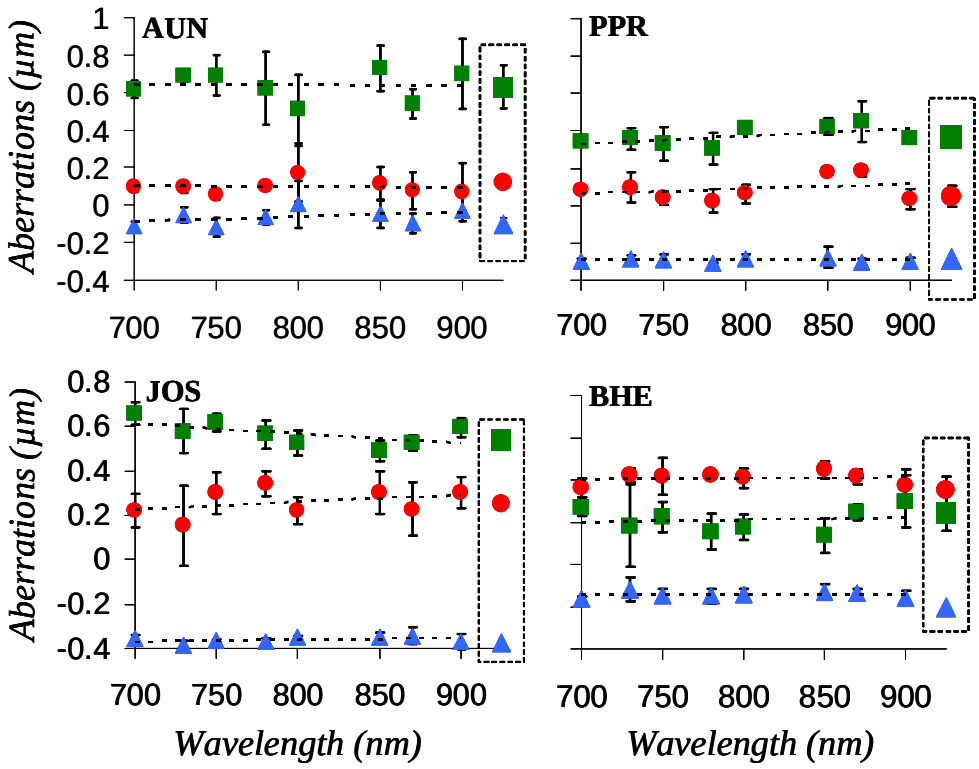

Fig. 3. Evolution of selected monochromatic aberrations (7 mm pupil size) as a function of wavelength. Squares: astigmatism; circles: coma aberration; and triangles: fourth order spherical aberration. The aberration estimates obtained for broad-band illumination are showed as larger points. The error bars show the standard deviation. The dashed lines correspond to the linear fit performed in each case.

To establish the possible evolution of these particular aberrations a statistical analysis was performed. Due to the relatively limited number of studied wavelengths, from a statistical point of view, we first performed a linear regression analysis. The linear fits are indicated in Fig. 3 by means of dashed lines. In most cases these lines are virtually flat, denoting no changes of the studied aberration term with wavelength. Even in the few cases where a slight slope can be noticed, the regression coefficient is low. As an example, the larger r^2 values obtained were 0.34 and 0.32 for astigmatism in subjects JOS and PPR respectively. Additionally, an Anova analysis was performed to calculate the probability, p, from the F-test at a 95% confidence level, showing no statistically significant relationship between

#6061 - $15.00 US Received 14 December 2004; revised 5 January 2005; accepted 5 January 2005

aberrations and wavelength in any subject. Following the former example, the obtained p-values for astigmatism in subjects JOS and PPR were 0.12 and 0.13 respectively.

In order to provide an estimation of the overall behavior of the aberrations as a function of wavelength in the NIR range, Fig. 4 presents the root mean square (RMS) of the wave-aberrations in each case. Defocus, which will be later studied separately, has not been included in the RMS. For all the subjects, a near plane linear fit of the RMS as a function of wavelength was found, again supporting the independence of the aberrations with wavelength. The r^2 coefficients were 0.07 for JOS, 0.04 for BHE, 0.0008 for AUN, and 0.36 for PPR. Although this latter subject exhibits a visible slope, there is no statistically significant association between RMS and wavelength (p-value 0.23). In Fig. 4 the results from the broad-band illumination measurements have been also included as independent, larger points. These results show that aberrations, beyond defocus, are nearly independent on the wavelength in the NIR range (700-900 nm).

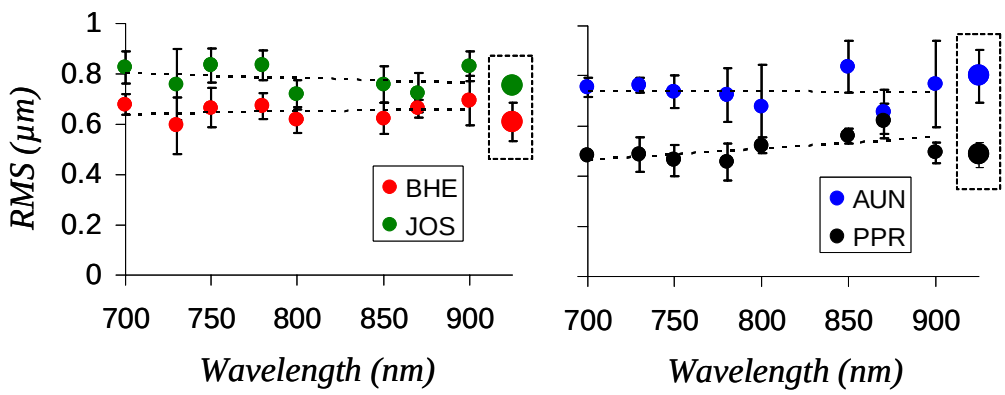

Fig. 4. RMS of the average ocular aberrations in the near IR band for each subject in a 7 mm pupil size. The defocus aberration was not included in the RMS. The dashed lines represent the linear fits. The obtained RMS when using the broad-band illumination (no interference filter) is showed with larger points for each subject.

We studied the change of defocus in the NIR range separately. Figure 5 shows defocus as a function of wavelength for every subject. The offset among curves is due to the individual level of refractive error of each subject. Nonetheless, the evolution of defocus among subjects is similar. After performing a linear regression, the r^2 parameter ranged from 0.92 to 0.95 in the four subjects. The Anova test showed the linear fit to be highly statistically significant in the four cases ($p = 0.00005$, $p = 0.0002$, $p = 0.00014$ and $p = 0.00009$ for JOS, BHE, AUN and PPR respectively).

Figure 6 presents the average defocus from the four subjects as a function of wavelength. Before averaging, the data were shifted along the vertical axis to cancel the defocus at the shortest wavelength (700 nm). Error bars correspond to the standard deviation calculated from the experimental set of data. The dashed line represents the linear fit, whose equation is:

$$\Delta R = 0.0021\,(\lambda\text{-}700) - 1.4341, \qquad (1)$$

where the units for ΔR (chromatic defocus with respect to 700 nm) and λ (wavelength) are diopters and nanometers respectively. In this case, the r^2 is 0.99, therefore supporting the use of the linear fit to the data. We found the linear equation (1) to be highly statistically significant following the F-test ($p = 0.00001$). Although this linear equation predicts the evolution of the defocus as a function of wavelength with high precision in the NIR range, it does not describe the physical process that produces this dependence. For the visible spectrum, chromatic defocus has been successfully modeled by using reduced schematic eyes, essentially accounting for the dispersion of water. The solid line in Fig. 6 shows the

#6061 - $15.00 US Received 14 December 2004; revised 5 January 2005; accepted 5 January 2005

predictions for chromatic defocus obtained by extending to the near IR range the equation previously proposed by other authors for the visible range [25]:

$$\Delta R = \frac{n_0 - n(\lambda)}{r \cdot n_D}, \tag{2}$$

where ΔR is the chromatic longitudinal aberration in the eye in diopters between the wavelength λ and the reference wavelength λo. The refractive index $n_D = 1.333$ corresponds to the emmetropic eye, following the proposed model (the subscript D refers to the 589 nm of the sodium line). It uses the Cornu's hyperbolic formula to model the refractive index of water [26]:

$$n(\lambda) = a + \frac{b}{(\lambda - c)}. \tag{3}$$

In this equation, we introduced the parameters obtained in the visible range by Thibos et al. [14]: a = 1.3205; b = 0.0047; c = 0.2141. In Fig. 6 the reference wavelength for Eq. (2) was 700 nm.

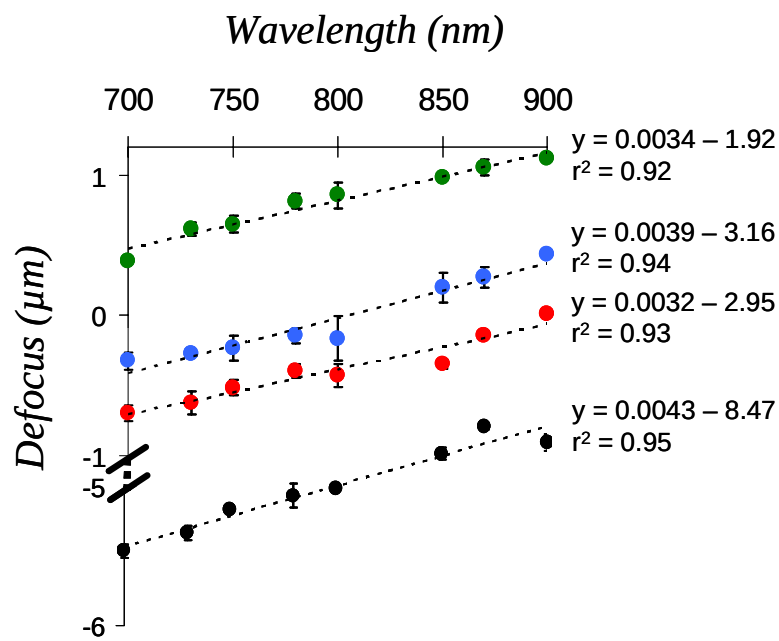

Fig. 5. Defocus (Zernike polynomial Z_4^0, 7 mm pupil size) as a function of wavelength. The linear fits are presented as dashed lines in each case. Each curve is labeled with the obtained linear equation together with the r^2 parameter. From top to bottom, the curves correspond to the subjects JOS, AUN, BHE and PPR. The error bars represent the standard deviation.

It has to be pointed out, that the mentioned parameters in Eq. (3) were obtained with a psychophysical method, so even in the visible range some discrepancy could be expected when comparing the results of this model with objective measurements of defocus. However, the experimental points from our measurements show a relatively good agreement with the extension of the water eye model obtained in the visible range. In particular, the ranges of variation are similar in both the experimental data and the extended water eye model. This good agreement apparently rules out other potential sources of chromatic defocus in the NIR. For example, since it is known that NIR light penetrates deeper in the retina than visible light,

#6061 - $15.00 US Received 14 December 2004; revised 5 January 2005; accepted 5 January 2005

a component of chromatic defocus could be speculated to arise from the reflection of different wavelengths at different retinal layers. However, our results do not support this hypothesis.

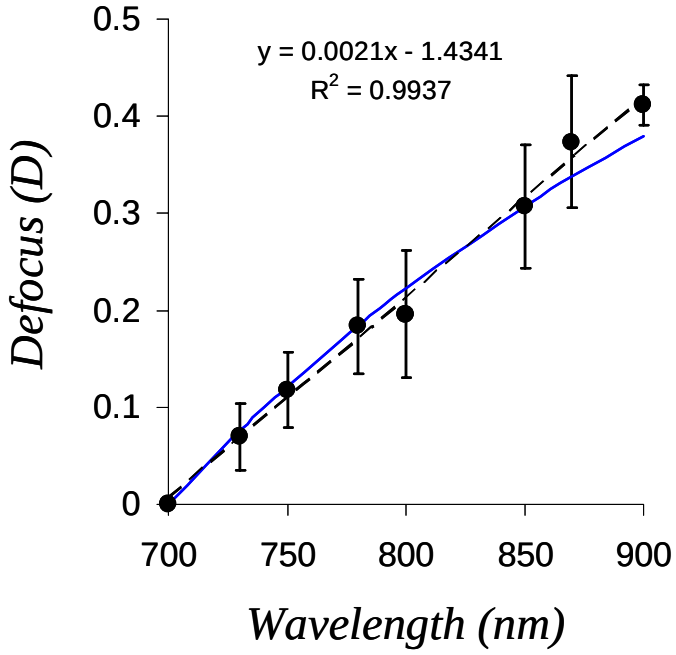

Fig. 6. Average chromatic defocus (D) from all the subjects as a function of wavelength in the near IR range (solid circles). The dashed line shows the linear fit performed to the average values while the blue solid line represents the extended water-eye model (see the text for more details) in the considered band. The obtained equation and the r^2 parameter from the calculated linear fit are also included on the figure. The error bars represent the standard deviation.

4. Conclusions

We have demonstrated the use of a pulsed laser, Kerr-lens mode-locked Ti:sapphire laser, for measuring the wave-aberrations with a Hartmann-Shack wave-front sensor in the NIR. The broad emission curve of the Ti:Sapphire femtosecond laser allowed us to systematically measure the eye's aberrations at several wavelengths in the NIR without switching the light source, so that the results are directly comparable.

With this tool, we have characterized the dependence of aberrations with wavelength in the NIR range. We found the ocular aberrations, excluding the defocus, to remain nearly stable with wavelength in the studied NIR range. The changes of defocus with wavelength in the NIR range were accurately fitted by a linear equation. In addition, a chromatic water eye model [14], although derived for the visible, also predicts well the behavior of defocus in the NIR.

The use of ultra-broadband laser sources is an excellent approach to study the ocular aberrations and perhaps other ocular parameters in the infrared. These sources, after adequately stretching the pulses, represent a promising alternative, especially if the cost of the system is reduced in the future, to the continuous wave (CW) laser sources in the study of the eye. Although we have presented in this work the use of a pulsed laser source in a Hartmann-Shack wave-front sensor, its use it is not limited to this particular sensor. The main advantage of using this type of broadband light sources is that wavelength selection can be easily performed by means of interference filters which can be obtained at any required wavelength, especially in the near IR band, without requiring multiple illumination channels with the associated difficulties in alignment. In particular, the optical properties of the retina in the

#6061 - $15.00 US Received 14 December 2004; revised 5 January 2005; accepted 5 January 2005

near IR range, where these sources are readily available, have not been investigated so far. The reflectivity, absorption and scattering processes in retinal tissues have not been characterized. The study of all these phenomena could be adequately accomplished by using this type of lasers.

From a practical point of view, the obtained results offer the possibility, for the first time to our knowledge, to systematically account for the chromatic defocus error in the large number of ophthalmoscopes currently working under NIR illumination, allowing comparison between devices using different wavelengths. Additionally, these results can be used in experiments where chromatic defocus wanted to be corrected, such as in imaging techniques using broad-band NIR light. In particular, a technique that can highly benefit from these findings is optical coherence tomography (OCT), where the use of broad-band IR illumination is mandatory. The results of this study support the approach of measuring and correcting the aberration for the center of the used band in adaptive-optics ultra-high resolution [27].

Acknowledgments

This work was supported by WF Y159-PAT and Christian Doppler Society, FEMTOLASERS, Inc. (Austria); "Ministerio de Educacion y Ciencia", grants BFM2001-0391, FIS2004-02153 (Spain) and ”Acción Integrada España-Austria”- HU2002-0011.